

## Drifting spatial structures in a system with oppositely driven species

K.-t. Leung<sup>1</sup> and R. K. P. Zia<sup>2</sup>

<sup>1</sup>*Institute of Physics, Academia Sinica, Taipei, Taiwan 11529, Republic of China*

<sup>2</sup>*Center for Stochastic Processes in Science and Engineering, Physics Department, Virginia Polytechnic Institute and State University, Blacksburg, Virginia 24061-0435*

(Received 3 February 1997)

A system consisting of two conservative, oppositely driven species of particles with excluded volume interaction *alone* is studied on a torus. The system undergoes a phase transition between homogeneous and inhomogeneous phases, as the particle densities are varied. Focusing on the inhomogeneous phase with generally unequal numbers of the two species, the spatial structure is found to drift counterintuitively against the majority species at a constant velocity that depends on the external field, system size, and particle densities. Such dependences are derived from a coarse-grained continuum theory, and a microscopic mechanism for the drift is explained. With virtually no tuning parameter, various theoretical predictions, notably a field-system-size scaling, agree extremely well with the simulations. [S1063-651X(97)09707-9]

PACS number(s): 64.60.Cn, 05.70.Fh, 66.30.Hs, 82.20.Mj

### I. INTRODUCTION

In the recent decade, there was considerable interest in the statistical mechanics of a variety of systems in stationary, but *nonequilibrium*, states. Notable examples include fast ionic conductors, surface growth, electromigration, flux creep in superconductors, propagation of defects and cracks, electrophoresis, and granular as well as traffic flow. Apart from practical applications, the interest lies in the need to establish a sound foundation for nonequilibrium statistical mechanics, on par with the Boltzmann-Gibbs formulation for systems in equilibrium. To pursue these goals, many authors have proposed simple models, just as Lenz and Ising did [1], in order to understand the phenomena of phase transitions of a magnet in thermal equilibrium. Along these lines, Katz, Lebowitz, and Spohn [2] introduced the simple *driven* Ising lattice gas, as an ‘‘entry’’ into the physics of nonequilibrium steady states. Since then, this field has steadily grown, so that there now exists many variations and generalizations of the proto model [3].

One of the most natural generalizations are systems with a second species of particles. The simplest of these is a model with *equal* numbers of oppositely ‘‘charged’’ particles, driven by a uniform external ‘‘electric’’ field and diffusing on a periodic, square lattice [4]. With *no* interparticle interactions, except the excluded volume constraint, this system exhibits a phase transition, for critical values of the particle density and external field, from a homogeneous disordered state with a sizable current to an inhomogeneous state with a minute current. Particles of the opposite charge impede each other and ‘‘lock up’’ into a dense region. By symmetry, the average location of this region is time *independent*. Since its inception, a number of its properties are reasonably well understood [5–8], while a variety of related ones have been proposed [9–11]. However, none of these studies focused on a system with *unequal* numbers of the two species. Assuming that a locked-up state still exists, one should not expect the dense region to remain stationary. In particular, we can expect a larger number of the majority species to lie within this region, and so, naturally expect the block to *advance*

*with the majority*. In this paper, we study such inhomogeneous states with both simulation and analytic techniques. Perhaps the most surprising of the results is that, in the ordered phase, the spatial structure, as a whole, drifts in a direction *opposite* to the intuitive picture above.

The remainder of this paper is organized as follows. In Sec. II, we provide specifications of this model and some details of the Monte Carlo runs. We present the simulation results of the counterintuitive motion of inhomogeneous states and suggest its microscopic mechanism in Sec. III. Section IV is devoted to the continuum mean-field approach, which was relatively successful in describing the charge-neutral model [4,6,7] and will be reanalyzed for the more general case here. These theoretical predictions are then compared to the simulation data in Sec. V. Particular attention will be paid to the scaling of the drive with the system size, and the dependence of the drift velocity on control parameters. We end with some concluding remarks in Sec. VI.

### II. A MODEL FOR DIFFUSION OF TWO, OPPOSITELY BIASED, SPECIES

Generalizing the work of Ising, Potts [12] and Blume, Emery, and Griffiths [13] introduced models which consisted of only three or more states per site in order to describe various systems such as magnets with spin one or higher and ternary mixtures. Along similar lines, the natural generalization of the driven Ising lattice gas [2] would be models of several species of particles, driven far from equilibrium by some ‘‘external’’ field. Clearly, there are many physical systems for which such models may be applicable. Here we will focus on the simplest one [4].

On a square lattice with  $L_x \times L_y$  sites, we place  $N_{\pm}$  particles with ‘‘charge’’  $\pm 1$ . At each site, there will be at most one particle, regardless of its charge. Thus a configuration of our model is completely specified by the set of occupation numbers  $\{n_{\pm}(x,y)\}$ , where  $n_{\pm}(x,y) = 1$  or 0, if there is a  $\pm$  particle at site  $(x,y)$  or not. Apart from this excluded volume constraint, there is no interaction between the particles. However, there is an external ‘‘electric’’ field  $E$ , cho-

sen to point in the  $+y$  direction, so that a  $+(-)$  particle is biased against moving in the  $-(+)$  direction. Specifically, the system evolves by random updating. In each trial, a pair of nearest neighbors is randomly chosen. If it is a particle-hole pair, then the particle hops into the hole with a probability  $\min\{1, e^{\pm E\hat{y}\cdot\hat{a}}\}$  for the  $\pm$  species, where  $\hat{a}$  denotes the direction of hopping.  $L_x \times L_y$  such trials constitute one time step (or one sweep). Finally, we impose periodic boundary conditions, so that our lattice is in fact a torus. For later convenience, let us define the terms ‘‘overall mass density’’ and ‘‘overall charge density,’’ given, respectively, by

$$m \equiv \frac{N_+ + N_-}{L_x L_y} \quad \text{and} \quad q \equiv \frac{N_+ - N_-}{L_x L_y}. \quad (1)$$

Clearly, for  $E=0$ , there is in fact no distinction between the two species. The system is purely diffusive and uninteresting. On the other hand, for  $E>0$ , particles of the opposite charge impede each other. This mutual blocking is so severe that the system displays drastically different characteristics if the particle densities are high enough. In all previous studies [4–6] of this model,  $q$  is restricted to zero for simplicity, so that there are only two control parameters ( $E, m$ ) besides the system size. There, for fixed  $E$ , say, the steady state of the system is disordered and homogeneous, provided  $m$  is small enough. By symmetry, the two opposing particle currents are the same, on the average. Thus the (average) hole current  $C$  is zero, while the (average) charge current  $J$  is nontrivial. As  $m$  increases,  $J$  increases sublinearly, as a result of the excluded volume constraint as well as the mutual blocking. Once  $m$  rises beyond a critical value  $m_c(E)$ , a phase transition occurs so that the system is ordered into an inhomogeneous state. In this state, three regions can be roughly identified: one particle-poor and two particle-rich zones, one of each species. As might be expected, these regions span the *transverse* dimension of the lattice ( $L_x$ ), with each particle-rich zone impeding the ‘‘forward motion’’ of the other species. For systems with  $O(1)$  aspect ratios, these zones are purely transverse to the drive, i.e., the densities are *homogeneous* in  $x$ . The current drops to vanishing values. If  $E$  is sufficiently large, this transition is extremely sharp and dramatic [4]. With larger aspect ratios, the system often locks up into somewhat different states, with zones spanning both  $x$  and  $y$ , i.e., wrapping around the torus with nontrivial winding numbers [5]. The current still suffers a drop, though not to vanishingly small amounts. In either case, once lock-up occurs, these zones are stationary on the average, since  $C=0$  always.

In this paper, we will study systems with *unequal* numbers of the two species. With  $q \neq 0$ , many of the previous properties will be different, although we still expect the presence of a phase transition. For example, in the homogeneous state,  $C$  will not vanish, and propagating fluctuations are possible. Deferring a comprehensive study of this model to a later publication [14], we will focus here only on the *inhomogeneous state*, in which the zones are expected to drift. As we will demonstrate and explain, the system displays a counterintuitive feature, i.e., the spatial structures drift in the direction favored by the *minority* species. For example, the inhomogeneities will drift in the negative  $y$  direction if  $q$  is positive.

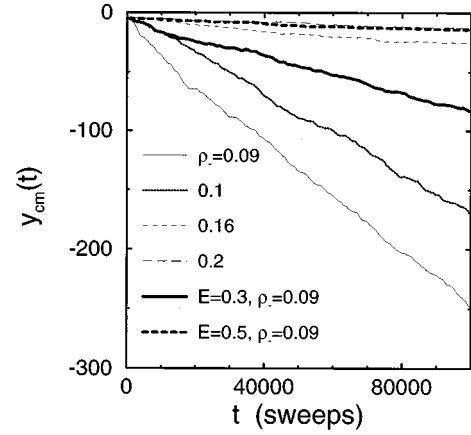


FIG. 1. The position of the center of mass  $y_{cm}$  vs time for the inhomogeneous state. The steady, backward drift velocity decreases with increasing average density of the minority phase.  $\bar{\rho}_+ = 0.25$  and  $E = 0.1976$ , except where otherwise stated.

### III. DRIFTING STEADY-STATE STRUCTURES FROM SIMULATIONS

Since our purpose here is to study the interesting properties associated with *unequal* numbers of the two species, we carry out simulations with fixed particle density ( $\bar{\rho}_+ \equiv N_+/L_x L_y$ ) for the  $+$  species and varying density for the  $-$  species ( $\bar{\rho}_- \equiv N_-/L_x L_y < \bar{\rho}_+$ ), corresponding to

$$q = \bar{\rho}_+ - \bar{\rho}_- > 0.$$

The behavior for the case of  $q < 0$  may be deduced simply by symmetry. Specifically, we choose  $\bar{\rho}_+ = \frac{1}{4}$ ,  $L_x = 10, 20,$  and  $40$ ,  $L_y = 40, 160,$  and  $320$ , and  $E$  ranging from about 0.1 to 1. These parameters are chosen in order to probe the  $q > 0$  region close to the  $q=0$  *inhomogeneous* states near the transition mentioned above, for we expect the properties to be more pronounced there. In contrast, the particles can hardly move deep in the locked-up phase at higher densities. Simulations for different  $L_x$ 's show that the effect of  $L_x$  is negligible, as found for the symmetric,  $q=0$  case [4]. Thus, unless  $L_x \gg L_y$  [5], which we will not consider here, we are dealing with a system in which only one of the dimensions plays an essential role.

Starting from the inhomogeneous state with  $\bar{\rho}_- = \bar{\rho}_+$ , we find a phase transition into a homogeneous state as we gradually decrease  $\bar{\rho}_-$  with  $\bar{\rho}_+$  held fixed. On the  $(q, m)$  plane, the phase boundary between the homogeneous and inhomogeneous states may be located this way, which is symmetric about the  $m$  axis. However, a detailed discussion of the phase diagram is beyond the scope of this paper.

Focusing on the properties of the  $q > 0$  inhomogeneous states, we find that the locked-up region of the two species drifts *backwards* with respect to the driving direction for the majority ( $+$ ) species at a definite velocity  $v$  that increases with  $q$  but decreases with  $E$ , as shown in Fig. 1. Figure 2 shows a typical inhomogeneous configuration in the steady state for  $q > 0$ . The steady-state ensemble averages of the local density profiles for the two species,  $\rho_+(y, t)$  and  $\rho_-(y, t)$ , are measured. Due to the drift, they are functions of



FIG. 2. A typical  $40 \times 160$  configuration in steady state showing the blockage between the two species. The open (filled) squares represent the upward (downward), or  $+$  ( $-$ ) drifting species. Note that there are more  $+$  particles escaping through the blockage to cause the structure to drift *downwards*. Here  $\bar{\rho}_+ = \frac{1}{4}$ ,  $\bar{\rho}_- = 0.1$ , and  $E = 0.1976$ .

$u \equiv y - vt$  alone. Figure 3 displays the steady-state density profiles for various values of  $q > 0$ .

To understand the microscopic mechanism for this backward motion, it is instructive to consider the role of holes inside the two particle-rich zones. The probability for a hole to diffuse against the drive into these zones from the outer zone boundaries is suppressed by  $E$  via  $e^{-E}$ . Thus, provided

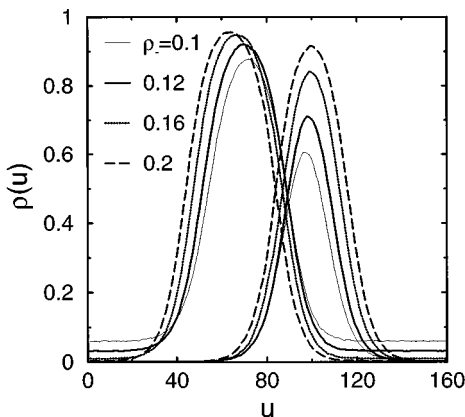


FIG. 3. Steady-state density profiles of a  $20 \times 160$  system for different  $\bar{\rho}_-$ , at fixed  $\bar{\rho}_+ = \frac{1}{4}$  and  $E = 0.1976$ .  $\rho_+(u)$  is on the left,  $\rho_-(u)$  is on the right, and  $u = y - vt$ .

$E$  is not too large, there are finite densities of holes inside the block. For  $q = 0$ , these densities are on the average the same in the  $+$  and  $-$  zone. For  $q > 0$ , there are more holes in the  $-$  zone because it is thinner (its thickness given roughly by  $\bar{\rho}_- L_y$ ). With holes available on the inner ( $+$   $-$ ) zone boundary, a particle may escape from the block to the particle-poor region through the zone of the *opposite* species. Driven along  $E$ , then, it eventually returns to the outer edge of its own zone due to periodic boundary conditions. When a particle leaves the inner zone boundary, a hole is left behind which may drift in either direction towards an outer zone boundary, returning to the hole-rich region. For  $q = 0$ , on the average, the number of holes impinging on an outer zone boundary equals the number of incoming particles. Thus, apart from a migration of particles from the inner to the outer zone edges, the cluster remains stationary. For  $q > 0$ , however, it is relatively easier for  $+$  particles to migrate. This results in more particles than holes impinging on the outer  $+$  zone boundary, and the opposite for the  $-$  zone. It is this imbalance that causes the whole cluster to drift backwards. Of course it is clear from our argument that  $v$  must vanish if  $E = \infty$ . In order to see how this arises theoretically and to explore the  $E$  and  $q$  dependence of  $v$ , we now turn our attention to a continuum description.

#### IV. CONTINUUM MEAN-FIELD DESCRIPTION

Following previous studies of this model [4–8], we rely on a mean-field-type continuum theory to understand the macroscopic properties here. The equations of motion for the densities, first proposed in Ref. [4], need no modification and, for completeness, are summarized below (Sec. IV A). However, the overall constraint on the charge density will be different, leading to qualitatively new behavior such as drifting inhomogeneous solutions (Sec. IV B).

##### A. Equations of motion

To describe the long-wavelength, low-frequency behavior of our model, we make use of the continuum approach, in which discrete variables of both the lattice and occupation numbers,  $n_{\pm}(x, y)$ , are replaced by continuous ones for the densities and space-time:  $\rho_{\pm}(\mathbf{r}, t)$ . For  $\mathbf{r}$ , we will continue to write  $(x, y)$ , which should not lead to any confusion, and let  $x \in [0, L_x)$ , etc. The evolution equations of these densities may be “derived” from the Master equation by taking the continuum limits of the “mean-field” approximation in which joint probabilities are factorized [10], or they may simply be postulated through considerations of symmetries. In the former approach, the parameters in the continuum equation can be related to the microscopic rates. Since we will not be concerned with the absolute time scale, one parameter may be absorbed into the definition of  $t$ . In other words, we will set the diffusion constant, for the *undriven* case, to be unity. Only one parameter remains, associated with the driving field. If the naive continuum limit approach is taken, then it is

$$\mathcal{E} \equiv 2 \tanh(E/2). \quad (2)$$

With these considerations, we study the following equations of motion, written in the form of continuity equations:

$$\frac{\partial \rho_{\pm}}{\partial t} = \nabla \cdot [\phi \nabla \rho_{\pm} - \rho_{\pm} \nabla \phi \mp \rho_{\pm} \phi \mathcal{E} \hat{y}], \quad (3)$$

where  $\phi \equiv 1 - \rho_+ - \rho_-$  is the density of holes, and  $\hat{y}$  denotes a unit vector along the  $y$  direction. Notice that the first two terms in these equations describe free diffusion of two distinguishable species of particles. The last term corresponds to the Ohmic currents, with  $\rho_{\pm} \phi$  being the usual density-dependent conductivity. It is also natural to consider the sum and difference of these equations. Defining  $\psi \equiv \rho_+ - \rho_-$  to be the charge density, they take the form

$$\frac{\partial \phi}{\partial t} = \nabla \cdot [\nabla \phi + \phi \psi \mathcal{E} \hat{y}], \quad (4)$$

$$\frac{\partial \psi}{\partial t} = \nabla \cdot [\phi \nabla \psi - \psi \nabla \phi - \phi(1 - \phi) \mathcal{E} \hat{y}]. \quad (5)$$

These are precisely the equations in Ref. [4]. To apply to our problem, we only need to impose

$$\frac{1}{L_x L_y} \int \psi dx dy = q > 0 \quad (6)$$

instead of  $q=0$ . The other constraint,

$$\frac{1}{L_x L_y} \int \phi dx dy = 1 - m, \quad (7)$$

as well as the periodic boundary conditions for the densities, of course, remain unchanged.

We may simplify these equations further, by absorbing  $\mathcal{E}$  into the scale of  $y$ . There is no need to write new equations, since we can simply drop  $\mathcal{E}$  from Eqs. (4) and (5) while keeping in mind that  $L_y$  must be replaced by  $\mathcal{E}L_y$ . That the drive provides an intrinsic length scale implies that the ordinary thermodynamic limit ( $L_y \rightarrow \infty$ ) must be taken along with  $\mathcal{E} \rightarrow 0$ , while holding the product  $\mathcal{E}L_y$  fixed. However, this simplification may be too confusing and will not be used here. Due to the central role played by  $\mathcal{E}L_y$ , let us define

$$\varepsilon \equiv \mathcal{E}L_y \quad (8)$$

for future convenience. Eqs. (4)–(7), completely specify the dynamics of our model.

### B. Inhomogeneous steady states

Next we study steady-state solutions to these equations which are spatially *inhomogeneous*. Since we expect the densities to be time dependent, let us seek solutions with a constant velocity,  $v$ , namely,  $\phi(x, y - vt)$  and  $\psi(x, y - vt)$ . Simplifying further, we note that all the states we observed in simulations are homogeneous in  $x$ , so that we will restrict ourselves to functions of the form

$$\phi(u) \quad \text{and} \quad \psi(u), \quad (9)$$

where  $u \equiv y - vt$ . Inserting these into Eqs. (4) and (5), we have

$$\begin{aligned} -v \partial \phi &= \partial [\partial \phi + \phi \psi \mathcal{E}], \\ -v \partial \psi &= \partial [\phi \partial \psi - \psi \partial \phi - \phi(1 - \phi) \mathcal{E}], \end{aligned}$$

where  $\partial$  stands for  $d/du$ . Integrating once, we obtain

$$\partial \phi + \mathcal{E} \phi \psi + v \phi = -C, \quad (10)$$

$$\phi \partial \psi - \psi \partial \phi - \mathcal{E} \phi(1 - \phi) + v \psi = -J.$$

The constants  $C$  and  $J$  may be interpreted as the two steady-state currents for the holes and the charges, respectively, in the *moving frame*. In the “lab frame,” the currents should be *inhomogeneous*, due to the anticipated drift of the block. As it stands, Eqs. (10) contain three unknown constants ( $v, C, J$ ), which will have to be fixed by three conditions, i.e., solutions be of period  $L_y$ , Eqs. (6) and (7). However, analytically, ( $v, C, J$ ) appear to play more the role of control parameters, while ( $L_y, q, m$ ) will emerge at the end. In this way, the analytic approach is somewhat opposite to that of simulations, where the latter (former) are the control (dependent) variables.

To find the solutions, we follow previous studies and introduce variables which simplify the structure of these equations:

$$\chi \equiv 1/\phi \quad \text{and} \quad \tilde{\psi} \equiv \psi \chi. \quad (11)$$

Note that, unlike the physical densities which are bounded,  $\chi \in [1, \infty]$  and  $|\tilde{\psi}| \leq \chi - 1 \in [0, \infty]$ . Now Eq. (10) becomes

$$\partial \chi = \mathcal{E} \tilde{\psi} + v \chi + C \chi^2, \quad (12)$$

$$\partial \tilde{\psi} = \mathcal{E}(\chi - 1) - J \chi^2 - v \tilde{\psi} \chi. \quad (13)$$

Eliminating  $\tilde{\psi}$ , we again arrive at an ordinary differential equation for only one variable:

$$\chi'' - (\chi - 1) + \hat{J} \chi^2 = \hat{v}^2 \chi^2 + \hat{C} \chi^3 + \left[ \hat{v} \chi \left( 1 - \frac{\chi}{2} \right) + \hat{C} \chi^2 \right]', \quad (14)$$

where  $\hat{J} \equiv J/\mathcal{E}$ , etc. Also, the prime denotes  $d/du\mathcal{E}$ , showing again the central role played by  $\mathcal{E}$  in setting the length scale. For clarity, on the right-hand side of this equation we have placed all the extra terms due to  $q \neq 0$ .

Unlike in the neutral system, the interpretation of Eq. (14) as a particle “moving” in a potential has to be modified, since there are “velocity” (i.e.,  $\chi'$ ) dependent “force” terms. In general, periodic “motion” would be impossible. Of course, here, we must insist on the existence of such solutions. The consequence is a constraint on the last term in Eq. (14). In particular, multiplying this equation by  $\chi'$  and integrating over the full period, we are led to  $\int (\chi')^2 [\hat{v}(1 - \chi) + 2\hat{C}\chi] du = 0$ . Since we are concerned with *inhomogeneous* states, we can expect  $(\chi')^2$  to be positive, except for isolated points. Thus it is possible to interpret  $(\chi')^2 du / \int (\chi')^2 du$  as a new measure on the interval  $u \in [0, L_y]$ , and define a type of average

$$\langle \dots \rangle \equiv \frac{\int \dots (\chi')^2 du}{\int (\chi')^2 du}. \quad (15)$$

Using this notation, we may write a simple relationship between the drift velocity and the hole current in the moving frame

$$v\langle\chi-1\rangle=2C\langle\chi\rangle. \quad (16)$$

Since typically  $\chi>1$ , we conclude that the drift is in the same direction as the hole current. A similar relationship can be found by integrating Eq. (12), after multiplication by  $\phi$ . The result is

$$-q\mathcal{E}=v+C\bar{\chi}, \quad (17)$$

where the bar is the normal average:

$$\bar{\dots}\equiv\frac{\int\dots du}{L_y}. \quad (18)$$

Eliminating  $C$  between Eqs. (16) and (17), we see that

$$\frac{v}{q\mathcal{E}}=-\left(1+\frac{\langle\chi-1\rangle\bar{\chi}}{2\langle\chi\rangle}\right)^{-1} \quad (19)$$

is negative definite. So, for example, if the majority species is positive (i.e., more particles are driven ‘‘upwards’’), then the drift of a block state will be ‘‘downwards.’’ This behavior is quite surprising, since we expect the particle-rich zone to contain more particles of the majority species, so that the entire block should ‘‘advance’’ with the majority. Instead, the block drifts in the *opposite* direction. On closer examination, we find that, since the negative region (in this example for  $q>0$ ) is thinner, it is easier for positive particles to penetrate the blockage. Then, due to the periodic boundary conditions, these particles pile up ‘‘behind’’ the positive region. As a result, the entire block appears to drift ‘‘backwards.’’ This picture simply provides another perspective on the intuitive arguments in Sec. III. Here we have proved that the structure ‘‘retrogrades.’’

Clearly, this analysis also leads to  $C/q$  being negative, i.e., the holes moving contrary to the majority species, which is hardly surprising. Before closing this subsection, we should comment on a number of other constraints on the three unknowns  $(v, C, J)$ , independent of the specific values of  $(L_y, q, m)$ .

In order to have any periodic solution at all, there must be some form of restoring ‘‘force’’ in Eq. (14). Examining the ‘‘potential’’ part of this ‘‘force,’’ i.e.,  $(\chi-1)-(\hat{J}-\hat{v}^2)\chi^2+\hat{v}\hat{C}\chi^3$ , we see that there would be no ‘‘well’’ to trap the particle, unless

$$\hat{J}>\hat{v}^2. \quad (20)$$

On the other hand, at least  $J-\hat{v}^2<\frac{1}{4}$  is needed, even in the neutral case. The cubic term further exacerbates the situation. The constraint that a ‘‘well’’ exists turns out to be

$$\hat{v}\hat{C}[4-18(\hat{J}-\hat{v}^2)+27\hat{v}\hat{C}]<(\hat{J}-\hat{v}^2)^2[1-4(\hat{J}-\hat{v}^2)]. \quad (21)$$

More information can be gleaned from regarding Eqs. (12) and (13) as flows in a ‘‘phase’’ plane. If a periodic solution exists, it would correspond to a closed loop and, by

continuity, there would be, generically, at least one focus (fixed point with spiral orbits) lying within. In order to have a *physical* solution, this fixed point must lie in the physical region:  $\chi\in[1, \infty]$  and  $|\bar{\psi}|\leq\chi-1$ . Since any fixed point must lie on the curve  $\bar{\psi}=-\hat{v}\chi+\hat{C}\chi^2$ , we obtain

$$(1+\hat{v})^2>-4\hat{C}. \quad (22)$$

Recalling that both  $\hat{v}$  and  $\hat{C}$  are negative, this confines both to be small quantities.

In our case, it is easy to check that there are three fixed points, one of which always lies outside the physical region. Of the remaining two, one is a focus and the other a saddle. Based on the characteristics of the neutral system, we expect our solution curve to run in between these two fixed points. Unlike the neutral case, however, the flow is not Hamiltonian in general and, in particular, the focus is not necessarily a center (i.e., eigenvalues corresponding to the flow linearized about the fixed point *not* necessarily purely imaginary). Thus, there is no guarantee that we can find a periodic solution. One possible scenario is that a unique limit cycle exists for *any* given  $(v, C, J)$ , provided they respect the inequalities (20) and (22). Another is that  $(v, C, J)$  satisfy a specific relation which allows for the existence of periodic solutions. A natural constraint to impose is that this fixed point be a center, with its associated eigenvalues being *pure imaginary*. This condition is equivalent to setting the coefficient of the last  $\chi'$  term in Eq. (14) to zero at that fixed point. This gives us an additional formula for the velocity,

$$v=\frac{2C}{1-\frac{1}{\chi^*}}, \quad (23)$$

where  $\chi^*$  denotes the fixed-point value of  $\chi$  at the center. Using Eq. (10), it is easy to see that the value of the densities at any fixed point satisfies a cubic equation with parameters  $(v, C, J)$ . Eliminating  $\chi^*$  by Eq. (23), we then obtain a quintic algebraic equation for  $v$  alone:

$$8\hat{C}_m^3+32\hat{C}_m^2\hat{v}+42\hat{C}_m\hat{v}^2+2\hat{J}\hat{C}_m\hat{v}^2+18\hat{v}^3+3\hat{J}\hat{v}^3-\hat{C}_m\hat{v}^4-2\hat{v}^5=0, \quad (24)$$

where  $C_m\equiv-v-C$  is the mass current in the moving frame. However, though this scenario guarantees periodic solutions at the lowest order in the neighborhood of the fixed point, we are unable to prove that, beyond the linear level, this condition is either necessary or sufficient for the existence of periodic solutions. There is, nevertheless, some numerical evidence that such solutions are available, as we will show in Sec. V. Equation (24) prescribes a surface  $v(C, J)$  in the  $C$ - $J$  plane. Subject to numerical uncertainties, we find that the parameters  $(v, C, J)$  generated by simulations indeed span a surface consistent with this scenario. Given the additional good agreement of the density profiles from numerical solutions and simulations in Sec. V, this latter scenario appears to be the more probable one.

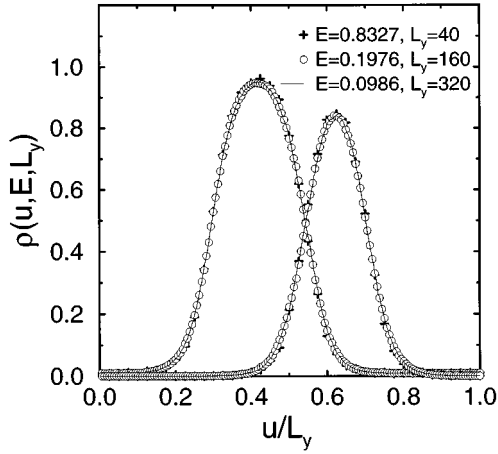


FIG. 4. Predicted field-size scaling is confirmed by simulations for different  $E$  and  $L_y$  with fixed  $\mathcal{E}L_y$ .  $L_x=20$ ,  $\bar{\rho}_+=\frac{1}{4}$ , and  $\bar{\rho}_-=0.16$ .

### V. FIELD-SIZE SCALING AND COMPARISONS WITH SIMULATIONS

To determine how closely the continuum model corresponds to the discrete model, we subject our theoretical predictions to the tests of simulations. The first is concerned with the scaling behavior in the system size and field strength. Choosing the alternative set of control parameters  $(L_y, q, m)$  in favor of  $(v, C, J)$ , Eqs. (12) and (13) imply that the solutions for the densities obey a simple scaling form (cf. [4,6,10]):

$$\chi(u, E, L_y, q, m) = \tilde{F}_\chi(\mathcal{E}u, \mathcal{E}L_y, q, m) = F_\chi(u/L_y, \mathcal{E}L_y, q, m), \quad (25)$$

where  $\tilde{F}_\chi$  and  $F_\chi$  are appropriate scaling functions. Similar scaling form holds for  $\psi$ , of course. Monte Carlo simulations, with fixed  $\bar{\rho}_+$  and varying  $\bar{\rho}_-$ , using a wide range of  $L_y$  and  $E$  with fixed  $\varepsilon = \mathcal{E}L_y$  show excellent agreement. An example is shown in Fig. 4. One immediate implication of this result is that the thermodynamic limit has to be taken with care, as phase transitions survive only in the double limits  $E \rightarrow 0$  and  $L_y \rightarrow \infty$  with  $\varepsilon$  held fixed.

A more stringent test is to check to what extent the data actually satisfy the differential equations (12) and (13). In the continuum description, it is more natural to use the currents in the moving frame because they are the integration constants. In simulations, the (spatial and temporal) average currents in the lab frame are more accessible. They are related. For example, the hole current in the lab frame is given by  $C + v\bar{\phi}$ , which is greater than  $C$ , in magnitude. With *no tuning parameter*, Eq. (12) for the hole density fits the data very well [see Fig. 5(a)], but there are appreciable discrepancies in Eq. (13) for the charge density in the particle-rich region [see the dashed line in Fig. 5(b)]. Similar discrepancies were also observed in a closely related model consisting of two species driven along orthogonal directions [10]. In that model, the asymmetry between the  $(+-)$  and  $(-+)$  nearest-neighbor correlations along the field direction was shown to give rise to additional cubic terms of the form  $\pm \lambda \rho_+ \rho_- \phi \mathcal{E} \hat{y}$  in the currents for the  $\pm$  species, which enter

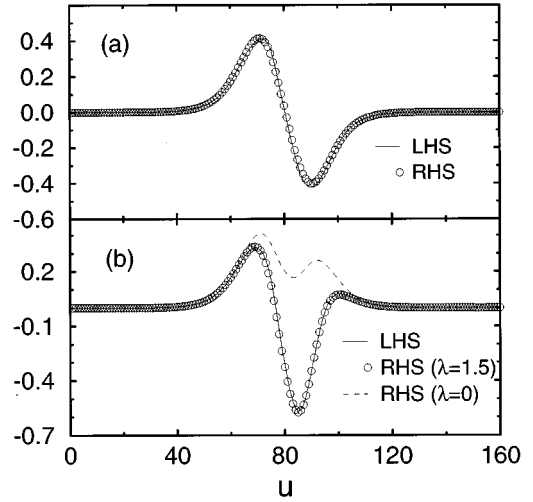


FIG. 5. Typical tests of local properties of the continuum model against simulations for (a) the hole equation (12), and (b) the charge equation (13), demonstrating the significance of the correction term  $\propto \lambda \mathcal{E} \rho_+ \rho_- \chi$  in the latter.  $L_x=40$ ,  $L_y=160$ ,  $E=0.1976$ ,  $\bar{\rho}_+=\frac{1}{4}$ , and  $\bar{\rho}_-=0.1$ .

inside the brackets on the right-hand side of Eq. (3). Due to the opposite signs, they cancel out in Eq. (4) for the hole (or mass) density but contribute an extra term to Eq. (5) for the charge density. These terms represent the lowest order corrections to our mean-field equations in Sec. IV. After such a term  $-2\lambda \mathcal{E} \rho_+ \rho_- \chi$  is added to the right-hand side of Eq. (13), significant improvements are found, for a suitable proportional constant  $\lambda$  [the solid line in Fig. 5(b)]. Notice that the value of  $\lambda$  may be estimated from the two-point density correlation functions [10].

Further comparisons are concerned with the mean current and drift velocity. The mass current  $-C - v\bar{\phi}$  in the laboratory frame, finite for  $q > 0$ , is simply given by  $\overline{\phi \psi \mathcal{E}}$ , which is obtained by integrating the first of Eqs. (10). Excellent agreement with simulations is found, as shown in Fig. 6(a). This comparison does not involve the  $\lambda$  correction terms. Other

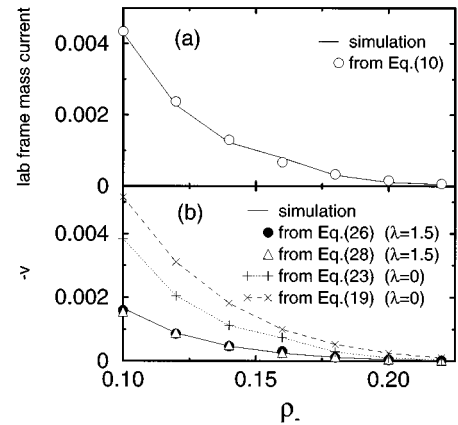


FIG. 6. Comparison between theory and simulation for (a) the mass current in the laboratory frame,  $-C - v\bar{\phi}$ , and (b) the (negative) drift velocity with and without the correction term, as a function of the average density of the minority species.  $L_x=20$ ,  $L_y=160$ ,  $E=0.1976$ , and  $\bar{\rho}_+=\frac{1}{4}$ .

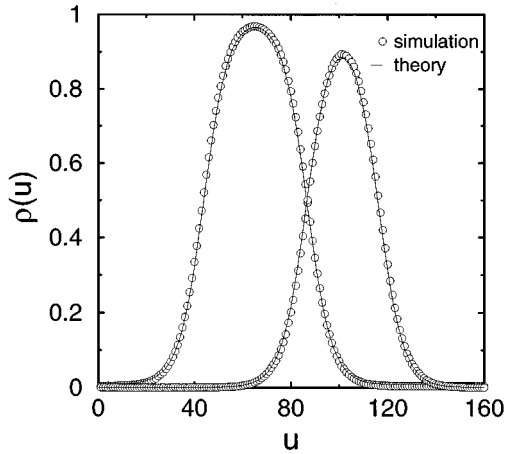


FIG. 7. Excellent agreement between theory and simulation for the density profiles.  $L_y = 160$ ,  $E = 0.1976$ ,  $\bar{\rho}_+ = 0.272$ ,  $\bar{\rho}_- = 0.184$ , and  $\lambda = 0$ .

predictions, such as Eqs. (19) and (23), derived by using both the hole and charge equations without  $\lambda$ , do not agree as well. Figure 6(b) exhibits increasing deviations as  $q$  increases. The agreement, however, can again be significantly improved by including the  $\lambda$  terms, with the same choice of  $\lambda \approx 1.5$  as in Fig. 5. With  $\lambda \neq 0$ , Eq. (19) is slightly modified:

$$\frac{v}{q\mathcal{E}} = - \left( 1 + \frac{2\lambda + \langle \chi - 1 \rangle_\lambda \bar{\chi}}{2(1-\lambda)\langle \chi \rangle_\lambda} \right)^{-1}, \quad (26)$$

where, similar to Eq. (15),

$$\langle \dots \rangle_\lambda \equiv \frac{\int \dots (\chi'/\chi^\lambda)^2 du}{\int (\chi'/\chi^\lambda)^2 du}. \quad (27)$$

Also, Eq. (23) becomes

$$v = \frac{(2-\lambda)C}{1 + \frac{\lambda-1}{\chi^*}}, \quad (28)$$

where  $\chi^*$  is approximated by the spatial maximum  $\chi_{\max}$  in Fig. 6, the error incurred is very small as both quantities are much greater than 1. Clearly, the  $\lambda$  terms play an important role, so that a good understanding of their origin is desirable. We have made some progress toward this goal, and measured several correlations as a confirmation. However, being beyond both the aim and the scope of this paper, these results will be deferred to another publication [14].

The final convincing evidence for the quantitative agreement is a direct comparison of the density profiles. For simplicity, we consider only the case of  $\lambda = 0$ . The fixed-point condition mentioned near the end of Sec. IV picks out a unique  $v$  for a given set of currents ( $J, C$ ) via Eq. (24). Equations (10) then contain no free parameter, and we can obtain the profiles by numerical integration, using for instance the Runge-Kutta method [15]. A typical comparison with the simulated profiles using the same set of parameters ( $q, m, L_y, E$ ) is presented in Fig. 7. The agreement for this case of a rather small  $q \approx 0.09$  is again excellent, even without  $\lambda$ . We expect more deviations for larger  $q$ , where the

$\lambda$  terms can no longer be ignored. These comparisons provide strong support to our claim that the continuum model, which may be systematically refined if necessary, represents a surprisingly accurate description of the simulated discrete model.

## VI. CONCLUDING REMARKS

To summarize, we studied, using both Monte Carlo techniques and the continuum mean-field method, a diffusive system of two species of particles, driven in opposite directions by an external field. With *periodic* boundary conditions imposed, this system settles into a *nonequilibrium* state with a steady current. For simplicity, we restricted ourselves to noninteracting particles, apart from an excluded volume constraint. Thus, as the particle densities increase, this system undergoes a phase transition, from a homogeneous disordered phase with a high current to an inhomogeneous one with minute current. In the latter state, the two species impede each other so much that they form a blockage of high, local-particle density. When the particle densities are *unequal*, this spatial structure displays a counterintuitive behavior. It drifts with a constant velocity, in a direction *opposite* to that favored by the majority species. Remarkably, simulation results agree reasonably well with most aspects of the theory, especially the prediction of  $\mathcal{E}L_y$  scaling. On the  $(q, m)$  plane, qualitative trends predicted by the linear stability lines of the homogeneous solutions to the mean-field equations (12) and (13) are also consistent with simulations.

On the other hand, there are clear signs of disagreement, mainly in connection with Eq. (13). Since our theory is based on mean-field assumptions, one avenue for improvement is to take some correlations into account. The simplest addition, involving cubic terms [10] in Eq. (3) lead to significant improvements. Encouraged by these findings, we are undertaking a comprehensive study, including a general phase diagram in the  $(q, m)$  plane, of the effects of such terms. In this paper, we focused only on the drifting inhomogeneous state. Although we performed some analysis for the *homogeneous* state [14], much remains to be investigated. For example, it would be desirable to observe, in simulations, the drift of fluctuations from the uniform densities. Of course, as in the neutral case, we should expect long-range correlations [8].

When restricted to one dimension (i.e., one column), this model is exactly solvable [16,17], since the order of any particular string of +’s and -’s is invariant, and no phase transitions can occur. With open boundary conditions, it can be mapped onto the Rubinstein-Duke model for electrophoresis [18], and more interesting phenomena can occur. Beyond the simple model studied here, there are many other generalizations which may be relevant to a variety of physical systems. We mention only a few here.

The existence of the inhomogeneous state depends crucially on the mutual blocking between the species. To find out the importance of this effect, we may introduce “charge-exchange” processes which take place at a fraction of the particle-hole exchange rate. As in the neutral case [11], we can expect to find the transition between the disordered and inhomogeneous states to be both continuous and discontinuous. It would be interesting to map out a complete phase diagram in the  $(\mathcal{E}L_y, m, q)$  space. Further, such a system can

display interesting behavior even in one dimension [19], especially with open boundaries [20]. In particular, it is closely related to the model of “first and second class particles” (e.g., cars and trucks) moving on a ring, in which a first class particle is allowed to overtake a second class one with some rate [21]. In that case, there are distinct phases, with properties reminiscent of our inhomogeneous states. The qualitative vs quantitative similarities should be investigated.

Another generalization involves the two species being driven in orthogonal directions. These models are motivated by the phenomena of traffic flow in city blocks and display a considerable variety of phases [9,10]. However, we believe that there are no studies with *unequal* numbers of the two species (though we are aware of a study with varying densities of a *third* species [22]). As we showed in this paper, it is likely that interesting behavior will be found if the species are not exactly balanced, which in view of the physical motivations should be the more generic cases to study.

In all the models mentioned so far, there is *no* interparticle interaction, except for the excluded volume constraint. It is clearly important to ask what the effects of including such interactions are. In particular, even in the absence of

external drives, there would be rich phase diagrams if interactions were present [13,12]. Thus, it is natural to inquire how the drive would modify these phase transitions. We are aware of only one study of a driven system with two interacting species [23]. Though the regime investigated was extremely limited, several interesting features were found.

Finally, we point out that, in physical systems such as fast ionic conductors, the two species may be of different mobilities and different “charges.” These properties add two dimensions to the phase space, leading to seemingly endless horizons for future explorations.

#### ACKNOWLEDGMENTS

We thank B. Schmittmann, S. Sandow, and S. Cornell for many stimulating discussions. One of us (R.K.P.Z.) is grateful for the hospitality of Academia Sinica (Taipei), where some of this work was carried out. This research was supported in part by grants from the National Science Council and National High Performance Computing Center of ROC, and the U.S. National Science Foundation through the Division of Materials Research.

- 
- [1] E. Ising, *Z. Phys.* **31**, 253 (1925).
  - [2] S. Katz, J. L. Lebowitz, and H. Spohn, *Phys. Rev. B* **28**, 1655 (1983); *J. Stat. Phys.* **34**, 497 (1984).
  - [3] B. Schmittmann and R. K. P. Zia, in *Phase Transitions and Critical Phenomena*, edited by C. Domb and J. L. Lebowitz (Academic, New York, 1995), Vol. 17.
  - [4] B. Schmittmann, K. Hwang, and R. K. P. Zia, *Europhys. Lett.* **19**, 19 (1992).
  - [5] K. E. Bassler, B. Schmittmann, and R. K. P. Zia, *Europhys. Lett.* **24**, 115 (1993).
  - [6] D. P. Foster, and C. Godrèche, *J. Stat. Phys.* **76**, 1129 (1994).
  - [7] I. Vilfan, R. K. P. Zia, and B. Schmittmann, *Phys. Rev. Lett.* **73**, 2071 (1994).
  - [8] G. Korniss, B. Schmittmann, and R. K. P. Zia, *Physica A* (to be published).
  - [9] O. Biham, A. A. Middleton, and D. Levine, *Phys. Rev. A* **46**, R6124 (1992).
  - [10] K.-t. Leung, *Phys. Rev. Lett.* **73**, 2386 (1994).
  - [11] G. Korniss, B. Schmittmann, and R. K. P. Zia, *Europhys. Lett.* **32**, 49 (1995); *J. Stat. Phys.* **86**, 721 (1997).
  - [12] R. B. Potts, *Proc. Camb. Philos. Soc.* **48**, 106 (1952); F. Y. Wu, *Rev. Mod. Phys.* **54**, 235 (1982).
  - [13] M. Blume, V. J. Emery, and R. B. Griffiths, *Phys. Rev. A* **4**, 1071 (1971).
  - [14] K.-t. Leung and R. K. P. Zia (unpublished).
  - [15] See, e.g., W. H. Press *et al.*, *Numerical Recipes*, 2nd ed. (Cambridge University Press, Cambridge, 1992).
  - [16] B. Derrida, *J. Stat. Phys.* **31**, 433 (1983).
  - [17] A. Kooiman and J. M. J. van Leeuwen, *Physica A* **194**, 163 (1993).
  - [18] M. Rubinstein, *Phys. Rev. Lett.* **59**, 1946 (1987); T. A. J. Duke, *J. Chem. Phys.* **93**, 9049 (1990); **93**, 9055 (1990).
  - [19] S. Sandow (unpublished).
  - [20] M. R. Evans, D. P. Foster, C. Godrèche, and D. Mukamel, *Phys. Rev. Lett.* **74**, 208 (1995); *J. Stat. Phys.* **80**, 69 (1995).
  - [21] B. Derrida, in *Statphys 19*, edited by B. Hao (World Scientific, Singapore, 1996).
  - [22] S. Mukherji and S. M. Bhattacharjee, cond-mat/9704217.
  - [23] M. Aertsens and J. Naudts, *J. Stat. Phys.* **62**, 609 (1991).